Environ. Sci. Technol. 1995, 29, 1059–1068

Behavior of Biofilters for Waste Air Biotreatment. 2. Experimental Evaluation of a Dynamic Model

MARC A. DESHUSSES,*,† GEOFFREY HAMER,‡ AND IRVING J. DUNN†

Biological Reaction Engineering Group, Chemical Engineering Department, Swiss Federal Institute of Technology (ETH), 8092 Zurich, Switzerland, and Department of Chemical Engineering, University College Dublin, Belfield, Dublin 4, Ireland

Experimental evaluation of a diffusion reaction model (part 1) for the determination of both steady- and transient-state behavior of biofilters for waste air biotreatment is presented. The model, applied to the aerobic biodegradation of methyl ethyl ketone (MEK) and methyl isobutyl ketone (MIBK) vapors from air as single and as mixed pollutants, proved appropriate for describing most of the experiments undertaken and served as a basis for comprehensive understanding of biofilter operation.

Introduction

In the first part of this paper (*1*), we presented and discussed the development and the parametric sensitivity of an innovative biofilter model for the description of both steady-state and dynamic biofilter operation. The model considered the biofilter to be divided into small ideally mixed subdivisions, and the dynamic mass balances for these were solved by finite difference. The model parameters were determined in a separate set of specific sorption and biofiltration experiments (*2*, *3*) so that further use of adjustable parameters was avoided, and predictive computation of biofilter operation was allowed. Beside conceptual explanation of the complexities of the biofiltration process, the approach presented offers a basis for biofiltration process optimization and biofilter design.

The purpose of this part is to experimentally evaluate the biofilter model for a number of selected typical operating conditions and to propose a conceptual explanation, based on model computations, of the phenomena that were observed. The aerobic biodegradation of methyl ethyl ketone (MEK) and methyl isobutyl ketone (MIBK) vapors in air during passage through compost-based biofilters served as the model system. The study of both steady-state and transient elimination of binary pollutant mixtures, assisted by advanced model simulations, provided a much greater scope for developing an understanding of biofiltration processes (*2*–*4*) than did more conventional approaches.

Materials and Methods

A schematic diagram of the equipment used is shown in Figure 1.

Biofilter and Packing Material. The biofilters were constructed from Plexiglas tubing and were 1 m in length and 8.0 cm in internal diameter. Column temperatures were maintained between 20 and 25 °C with either external liquid circulation or electrical thermostatic jackets. Both thermostatic systems allowed the sampling at various column heights. The sample ports were located at 0, 25, 50, 75, and 100% of the total column height.

The biofilters were filled with Bioton, a commercially available biofilter packing (ClairTech, Utrecht, The Netherlands), comprising an equivolume mixture of compost and polystyrene spheres. Acid-neutralizing components (probably limestone) were also included in the biofilter material, but no activated carbon was incorporated. The voidage of the packing material, determined by studying the residence time distribution after a pulse of inert gas, was 50% (*3*). The active filter bed height was between 0.8 and 0.95 m for most experiments, and the packing density (60 wt % water content) was between 220 and 330 g of packing/L of bed volume. Before use, the packing material was inoculated with a concentrated enrichment culture. No additional mineral nutrient source was added after beginning the experiments.

* Address correspondence to this author at his present address: College of Engineering, University of California, Riverside, Riverside, CA 92521.

† Swiss Federal Institute of Technology.

‡ University College Dublin.

0013-936X/95/0929-1059$09.00/0

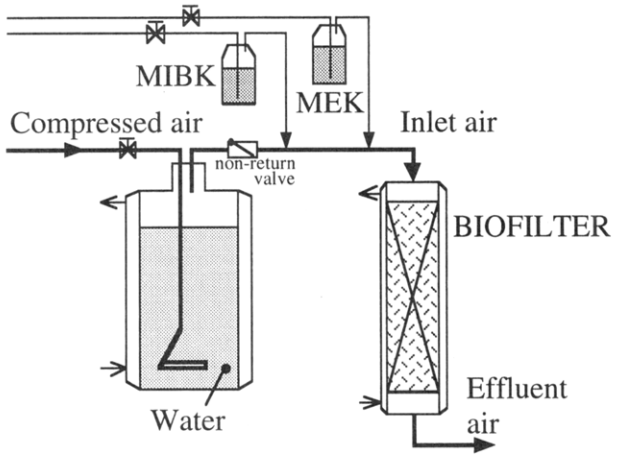

FIGURE 1. Schematic diagram of the equipment used.

Inoculum. Ketone-degrading enrichment cultures were grown in a mineral medium with MEK, MIBK, or mixtures of MEK/MIBK as the sole carbon and energy substrate(s) with regular transfers. The initial source of microorganisms was in samples from several wastewater treatment plants and soils. Samples subjected to a high level of aeration were preferred. The enrichment cultures showed extensive growth on either MEK and MIBK or mixtures of the two substrates. The packing material inoculum was prepared by concentrating 3 L of enrichment culture to 0.02 L by centrifugation. This was sufficient to coat 1 kg of packing material prior to its introduction into the columns.

Pollutant-Containing Humid Airstream. Compressed oil-free air was saturated with water vapor by sparging the air through a 50-L bottle containing deionized water thermostated at 28 °C. Two smaller compressed airstreams were sparged into 0.5-L bottles, containing either MEK and MIBK as required, and subsequently mixed with the major humidified airstream. The main airstream was regulated by mass flow meters (Brooks, The Netherlands). Non-return valves were installed in order to prevent contamination of the humidifying section with pollutant vapors. A metered flow of pollutant-containing humid air was passed downward through the biofilter.

Operating Conditions. Downward gas flow rates of 0.2 and 0.4 $m^3 h^{-1}$ were used most of the time, giving a surface loading of 40 and 80 m h^{-1} and a volumetric loading of 44 and 88 h^{-1}. The gas had a relative humidity greater than 95%, and the pressure drop over the filter was less than 50 mm by water gauge. Between each set of steady-state measurements, the biofilters were allowed to stabilize for at least 2 days, after which time no changes in pollutant removal characteristics could be observed.

Analysis. The concentrations of MEK and MIBK in the gas phase were determined by gas chromatography. Polluted air was pumped through 0.1-mL sampling loops for automatic injection into a Hewlett Packard type 5890A gas chromatograph fitted with a 15-m HP-50+ column and operated isothermally at 45 °C. The carrier gas used was helium (2.25 L h^{-1}) and detection was with a flame ionization detector. The detection limit was ca. 0.005 g of pollutant/m^3 of air. The retention times were 0.7 and 1.7 min for MEK and MIBK, respectively. The use of known airflow rates and both MEK and MIBK mass flow rates allowed the calibration of both systems.

Results and Discussion

In the present study, model predictions are compared with experimental results under steady-state and dynamic conditions. The model predictions are based on the model presented earlier (1) using the parameters listed in Table 1.

Results are presented in several forms, but are normalized to allow direct comparison with other published work. Removal, as strictly defined, is the percent conversion of pollutant expressed by eq 1.

$$\text{removal} = \frac{\text{inlet} - \text{outlet concentration}}{\text{inlet concentration}} \times 100\% \qquad (1)$$

The volumetric loading is defined as the ratio of the gas flow rate, G, to the total biofilter bed volume as expressed in eq 2. Equation 3 defines the pollutant load, which represents the normalized amount of pollutant entering the biofilter.

$$\text{volumetric load} = \frac{G}{\text{biofilter bed volume}} \qquad (\text{m}^3\ \text{m}^{-3}\ \text{h}^{-1}) \quad (2)$$

$$\text{pollutant load} = \frac{G \times \text{inlet concentration}}{\text{biofilter bed volume}} \qquad (\text{g}\ \text{m}^{-3}\ \text{h}^{-1}) \quad (3)$$

Similarly, the elimination capacity is the quantity of pollutant degraded per cubic meter of biofilter bed volume:

$$\text{elimination capacity} = \frac{(\text{inlet} - \text{outlet concentration})\ G}{\text{biofilter bed volume}} \qquad (\text{g}\ \text{m}^{-3}\ \text{h}^{-1}) \quad (4)$$

Further, the critical load is defined as the minimum pollutant loading for which the biofilter reaches its maximum elimination capacity.

Steady-State Performance. Steady-state features can be described using the dynamic biofilter model by running a simulation until stationary conditions are reached. To determine the steady-state characteristics of a biofilter, several simulations are required.

MEK Removal. Figure 2 compares experimentally determined elimination capacities to model predictions for the removal of MEK as a single pollutant at two different airflow rates, 0.20 and 0.40 $m^3 h^{-1}$, i.e., volumetric loadings of 44 and 88 $m^3\ m^{-3}\ h^{-1}$, respectively. While excellent agreement for the lower flow rate tested is observed, significant differences between the model and the experiments are evident at the higher flow rate tested. It is also evident that only slight differences between the two model computations occur in the intermediate domain, i.e., at loadings about 100−150 g $m^{-3}\ h^{-1}$. At higher loadings, the model indicates maximum degradation and a constant elimination capacity of 121 g $m^{-3}\ h^{-1}$.

MIBK Removal. In a similar manner, model predictions for MIBK are presented and compared with experimental results in Figure 3. Experimental data and model computations are found to be in reasonably good agreement. However, in the intermediate range, i.e., at a loading of 40 g $m^{-3}\ h^{-1}$, the model significantly overestimates the biodegradation capacity of the system. Several explanationsexist for this deviation, but the most plausible is that the kinetics used do not adequately describe the substrate uptake in this concentration range. The maximum elimination predicted is about 30 g $m^{-3}\ h^{-1}$.

TABLE 1

Model Parameters for Simulation of Elimination of MEK and MIBK in Biofilters (*1*–*3*)

biofilter characteristics	symbol	value	unit	source
interfacial area per volume unit	A	150	$m^2\ m^{-3}$	adapted from ref 5
biofilm thickness (sorption volume not counted)	Z	100	μm	adapted from ref 5
porosity of the filter bed	ϵ	0.5		mean residence time studies of pulses of inert gas in the biofilter bed (*3*)
moisture content of the packing material	mc	60	wt %	drying of weighed packing samples (*3*)

		value			
pollutant characteristics	symbol	MEK	MIBK	unit	source
effective diffusion coefficient	D	2.85×10^{-10}	5.37×10^{-10}	$m^2\ s^{-1}$	model fitting of sorption experiments on inactive packing material (*3*)
maximum degradation rate	V_m	22.5×10^{-4}	5.51×10^{-4}	$kg\ m^{-3}\ s^{-1}$	model fitting of independent single pollutant degradation experiments in biofilters (*3*)
Michaelis–Menten constant	K_m	1.37×10^{-3}	1.49×10^{-3}	$kg\ m^{-3}$	model fitting of independent single pollutant degradation experiments in biofilters (*3*)
competition-inhibition constant	K_i	3.70×10^{-4}	1.32×10^{-3}	$kg\ m^{-3}$	model fitting of independent mixed pollutant degradation experiments in biofilters (*3*)
Henry coefficient	H	2.35×10^{-3}	5.71×10^{-3}		direct GC measurements of gaseous and aqueous phase concentrations (*3*)

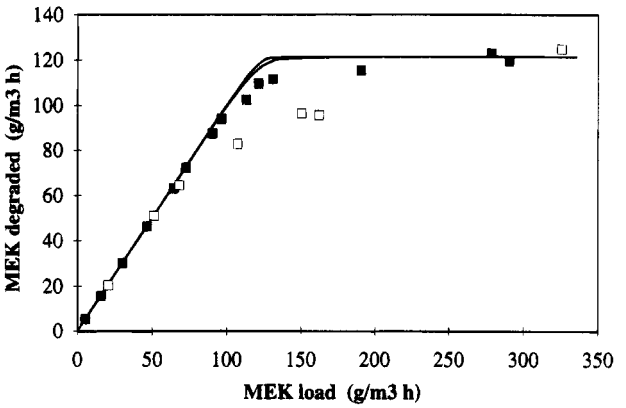

FIGURE 2. Comparison of predicted elimination/loading characteristics (lines) and experimental results for MEK removal as single pollutant, 0.20 $m^3\ h^{-1}$ (■), and 0.40 $m^3\ h^{-1}$ (□).

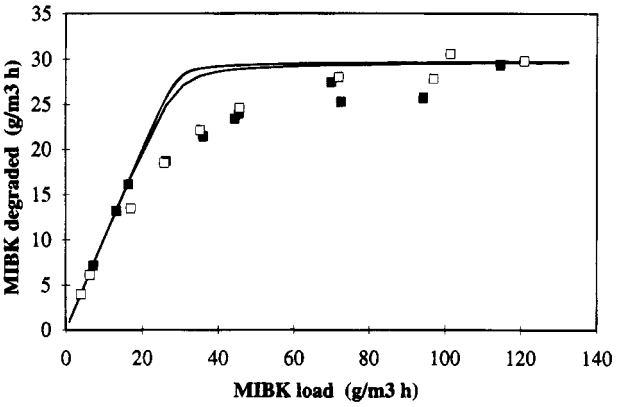

FIGURE 3. Comparison of predicted elimination/loading characteristics (lines) and experimental results for MIBK removed as single pollutant, 0.20 $m^3\ h^{-1}$ (■), and 0.40 $m^3\ h^{-1}$ (□).

MEK and MIBK elimination characteristics as single pollutants reported in Figures 2 and 3 exhibit significant differences. Both breakthrough concentrations and maximum elimination capacities were markedly superior for MEK removal than they were for MIBK removal. Several explanations exist concerning these significant differences. First, the microbial utilization rate of MEK is expected to be notably higher than that for MIBK (*6*–*8*). Second, the differences in solubilities, in vapor pressures, and consequently in their Henry coefficients are probable factors leading to more effective removal of MEK. Kirchner *et al.* (*9*) and Wolff (*10*) have emphasized that the difficulty in removal particular chemical vapors increases with their Henry coefficients, especially when the dimensionless Henry coefficient is higher than 10^{-3}, which is the case for both MEK ($H = 2.35 \times 10^{-3}$) and MIBK ($H = 5.71 \times 10^{-3}$). Such a dependency of effective removal on the Henry coefficient can be understood by considering the decrease in interfacial concentration, i.e., the maximum biofilm concentration obtainable, with increases in the Henry coefficient. A marked difference in the maximum operating concentration will be seen by the process culture, and this will be reflected by a consequential reduction in the biodegradation rate.

Simultaneous Removal of MEK and MIBK. As far as the biodegradation of VOCs in industrial biofilters is concerned, it is complex mixtures of pollutants that are most commonly encountered. Therefore, features concerning the removal of multiple pollutants require investigation.

Mixtures containing equal concentrations of MEK and MIBK vapor were studied with respect to their removal at two airflow rates in experiments similar to those reported previously for the individual removal of each individual pollutant. The elimination characteristics specific to these operating conditions are reported in Figure 4, where it is obvious that the biofilter was much more effective in removing MEK than it was in removing MIBK. In Figure 4, results for two flow rates are reported. Good correlation between each individual elimination at the two flow rates was observed. It is evident that, as reported above for the removal of MIBK alone, equal loadings lead to equal degradation rates. In both cases, MIBK elimination was less than half that for MEK, and the elimination capacity for MEK did not reach a distinct maximum during the experiment. However, a value of ca. 40–42 $g\ m^{-3}\ h^{-1}$ was the estimated maximum. The maximum MIBK elimination capacity was found to be 18 $g\ m^{-3}\ h^{-1}$ for loadings of about 50 $g\ m^{-3}\ h^{-1}$, although a slight decrease in MIBK degradation activity was observed at higher loadings. The most plausible explanation for this is that MEK more effectively inhibits MIBK biodegradation with increasing pollutant

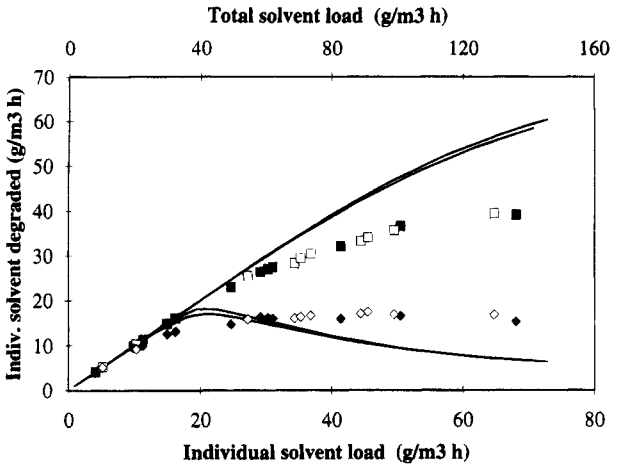

FIGURE 4. Modeled (lines) and experimentally determined (symbols) degradation characteristics for the biofiltration of equal concentration mixtures of MEK and MIBK at volumetric loadings of 44 $m^3 m^{-3} h^{-1}$: MEK (■) and MIBK (♦) and 88 $m^3 m^{-3} h^{-1}$: MEK (□) and MIBK (◇).

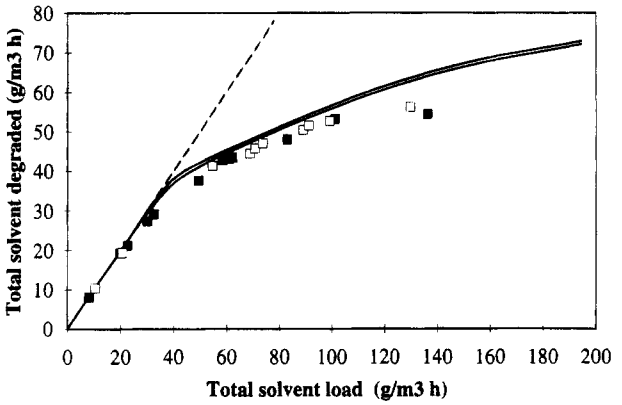

FIGURE 5. Modeled (solid lines) and experimental (■ and □) degradation characteristics for the total amount degraded at each volumetric loading, 44 (■) and 88 $m^3 m^{-3} h^{-1}$ (□). The dashed line represent complete removal of both ketones.

loading. Earlier pulse experiments substantiated this conclusion (*3*).

Results for the overall performance of the biofilter are shown in Figure 5, where the total amount of substrate removed corresponds to that achieved in Figure 4. The characteristic curve obtained shows a relatively large transitional domain, after which a maximum of 55 g m^{-3} h^{-1} total pollutant degraded was reached.

As far as model predictions for systems removing mixtures of MEK and MIBK are concerned, Figures 4 and 5 show that agreement between model and experiment is less satisfactory than for single pollutant removal. Systematic deviations between experimental and modeled values are observed for MEK, while MIBK degradation is overestimated below the critical loading and underestimated above the critical loading. The model computations drawn in both Figures 4 and 5 for both flow rates show that they lead to essentially the same amount of pollutant degraded at both volumetric loadings.

As far as the total amount degraded is concerned, Figure 5 indicates reasonable agreement between the model and experiments. Both complete removal and intermediary domains are appropriately described by the model, with significant deviation occurring only at the highest loadings tested.

Table 2 compares some experimental results with the corresponding computed values and underlines both the

TABLE 2

Experimental Results and Model Predictions for Selected Operating Conditions for Biofilters Removing MEK and MIBK from Mixtures with Equal Inlet Concentrations

	experiment	predicted[a]
MEK Breakthrough Inlet Concentration (g m^{-3})		
volumetric loading = 44 $m^3 m^{-3} h^{-1}$	0.45 ± 0.05	0.64
volumetric loading = 88 $m^3 m^{-3} h^{-1}$	0.20 ± 0.04	0.31
MIBK Breakthrough Inlet Concentration (g m^{-3})		
volumetric loading = 44 $m^3 m^{-3} h^{-1}$	0.25 ± 0.02	0.31
volumetric loading = 88 $m^3 m^{-3} h^{-1}$	0.09 ± 0.02	0.11
Maximum Pollutant Degraded (g $m^{-3} h^{-1}$)		
MEK	40 ± 1	>60[b]
MIBK	18 ± 1	18[c] 5[d]
Maximum Total Inlet Concentration To Comply with Swiss Regulations[e] (g m^{-3})		
volumetric loading = 44 $m^3 m^{-3} h^{-1}$	0.88 ± 0.01	1.09
volumetric loading = 88 $m^3 m^{-3} h^{-1}$	0.62 ± 0.01	0.64

[a] Predicted breakthrough is considered to occur when the computed outlet concentration equals 0.002 g m^{-3}. [b] No maximum in the degradation was predicted within the selected range of operating conditions. [c] Local maximum elimination capacity for a loading of ca. 20 g of MIBK $m^{-3} h^{-1}$. [d] Final value of the maximum loading tested. [e] Maximum exhaust air concentration of 0.15 g m^{-3}.

systematic overestimation of biofilter efficiency and the relatively inexact quantification of MEK/MIBK interaction at high concentrations. Even so, application of the model in the lower concentrations and the lower loading domain is entirely satisfactory, and close agreement between the experimental results and the predicted values are obtained.

The above examples and discussion prove that steady-state removal features can be reasonably predicted by the biofilter model developed herein. The model simulation proved accurate in describing both single pollutant and mixed pollutant removal over a wide range of sensible operating conditions. Design experiments that would quantify more precisely the exact nature of both the uptake and the competition kinetics are required in order to improve the reliability of the model.

Concentration Profiles in Biofilters. As far as the biodegradation of pollutant mixtures in biofilters is concerned, very little information exists on concentration profiles within the biofilter bed. Previous discussion (*4*) stressed the relative inadequacy of published biophysical models particularly with respect to the description of entire concentration profiles during the multicomponent removal operating mode. Hence, experiments where biofilter concentration profiles were studied (*4*) with respect to different airflow rates are compared with model predictions. Furthermore, the model is used to describe gradients that are expected to occur in the active biofilm. Experiments where the pollutant concentrations in the inlet airstream were kept constant at 0.30 g m^{-3} MEK and 0.33 g m^{-3} MIBK, giving a total substrate concentration of 0.63 g m^{-3}, were modeled as described above. Airflow rates ranged (*4*) from 0.15 to 0.47 $m^3 h^{-1}$, giving a surface loading of 30–95 $m^3 m^{-2} h^{-1}$ and a volumetric loading of 35–111 $m^3 m^{-3} h^{-1}$.

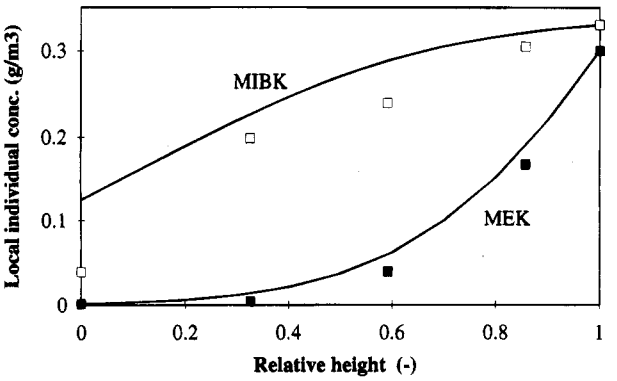

FIGURE 6. MEK (■) and MIBK (□) concentration profiles as a function of the relative sampling height at a polluted airflow of 0.34 $m^3 h^{-1}$. Because of the down-flow mode of operation, the inlet is located at a relative bed height of 1. The lines represent model predicted profiles.

The gaseous concentration profiles reported in Figure 6 reveal that simultaneous biodegradation of the two ketones occurred, although effective MIBK removal was only achieved after significant MEK removal. Reasonable agreement between the experimental values and the predicted profiles is observed.

In addition to the determination of axial gaseous concentration profiles, the biofilter model developed herein can provide valuable information on concentrations in the active biofilm. Previously, no experimental data have been reported for such profiles measured in real systems. The modeling approach proposed herein can thus be considered as an alternative to complex measurements for developing a conceptual understanding of the active biofilm environment. The model developed (*1*) assumed that the biofilter was divided into 10 layers, each comprising a gas phase; a biofilm; and a sorption volume, with the biofilm split into four subdivisions. In the following analysis, the computed concentrations for the interface, the four biofilm subdivisions, and the sorption volume are represented over the entire biofilter height. The results for the simultaneous removal of MEK and MIBK at 0.15 and 0.34 $m^3 h^{-1}$ under the operating conditions defined previously are shown in Figure 7. At the lower flow rate (top part of Figure 7), significant concentration gradients can be seen both in the axial direction and within the biofilm. MEK is readily depleted and from layer five onward does not penetrate the entire biofilm. MIBK shows similar behavior, but as it competes with MEK for biodegradation. As both its rate of biodegradation is slower and its effective diffusion coefficient is higher than those for MEK, it is eliminated only in the eighth layer. Moreover, MIBK biofilm gradients are found to be less pronounced than those for MEK. It can also be seen that concentrations in biofilm cell four and in the sorption volume are equal, which is a condition for steady state according to the differential equations of the model (*1*).

The graphs at the bottom of Figure 7 provide concentration data for a polluted airflow rate of 0.34 $m^3 h^{-1}$. With increasing airflow rate, the penetration concentration profile increased in both the axial and biolayer directions. MEK still exhibits significant gradients in the biofilm, but this is no longer the case for MIBK. This is due to differences in the ratio of reaction rates to the diffusion rates for MEK and MIBK.

The above figures and associated discussion emphasize the importance of the local concentration gradients encountered in both active biofilms and the sorption volume. Accordingly, similar heterogeneities are encountered in the local biodegradation rate (*3*, *4*), and these have major consequences on local elimination capacities. The existence of significant, nonlinear, gradients in both the biofilm and the biofilter height is a source of major complication with respect to the determination of biodegradation kinetics. Here, the simplified approach (*11*), where a uniform concentration in the liquid phase is assumed, hereby allowing the use of the Michaelis–Menten type relationship based exclusively on gaseous concentrations to describe the elimination characteristics, should not be used. Such an approach must be restricted to a first approximation design calculation for a bioscrubber (*12*) where the presence of a well-mixed, free-liquid phase permits a uniform biofilm concentration to be considered. Even so, it does not permit any detailed understanding of the complex interactions involved to be developed. In the present case, the fact that the reaction rate order changes within the range of practical interest, depending on the operating mode and conditions, justifies the use of nonlinear kinetic relations without simplification of either first- or zero-order kinetics.

Dynamic Behavior of Biofilters. Industrial biofilters are exposed both to effluent airstreams from continuous processes, when the waste air composition is usually relatively constant, and waste airstreams from discontinuous processes, in which variable conditions are frequently observed. Previously, little has been published on the transient response of biofilters. This section deals with some typical responses that may occur in real systems, particularly step changes in inlet concentrations and in airflow rates.

Step Changes during Single Pollutant Elimination. An experiment in which the airflow rate was maintained constant at 200 $m^3 h^{-1}$, i.e., a volume load of 44 $m^3 m^{-3} h^{-1}$, with MEK as the sole pollutant in the inlet airstream was varied stepwise is illustrated in Figure 8.

After both step changes, about 2 h was needed in order to reach a new steady state. Due the influence of sorption onto the packing, a delay of ca. 0.5 h was observed between each step change and significant changes in the outlet concentration of MEK. In no case did the outlet concentration overshoot the corresponding value for stationary operation. This indicates that the process culture was subjected to neither inhibition as a result of pollutant shock, which would have caused a temporary loss in removal activity, nor any subsequent net biomass build up. The lines in Figure 8 represent model predictions that are in close agreement with the experimental data. Even so, during transitions, the model predicts significantly lower outlet concentrations than those observed, probably as a result of incorrect description of sorption kinetics by the model.

The experiment reported in Figure 9 combines both concentration and airflow rate step changes. The entire experiment was performed in the concentration domain where the model predicted no breakthrough (see Figure 3), i.e., in the domain where the major differences between model and experiment are observed. For this reason, no comparison with the simulated concentration outlet was possible. However, simulated intermediary concentrations within the biofilter bed are illustrated.

After the first step change at 4.3 h, an hour-long breakthrough was observed before complete removal

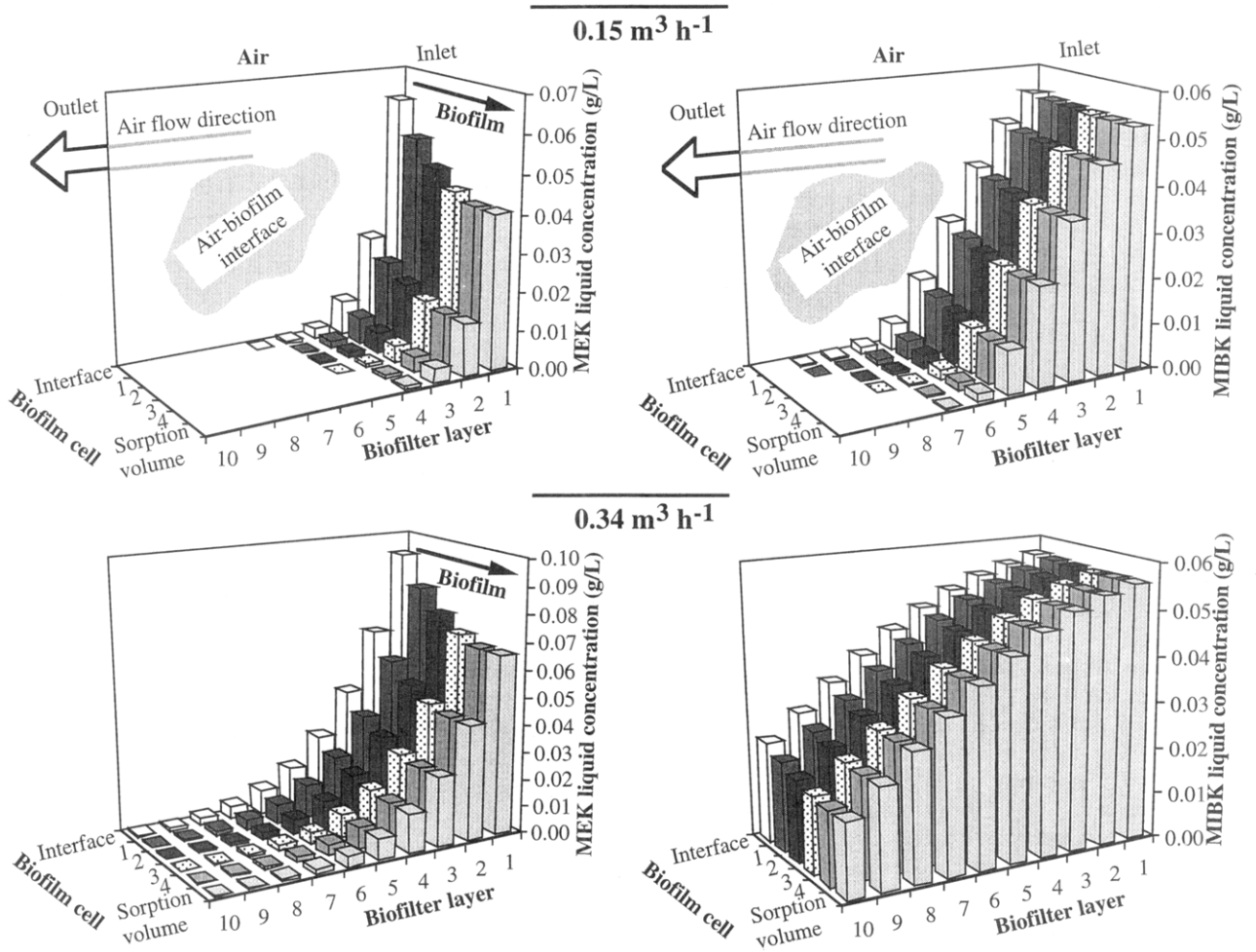

FIGURE 7. Three-dimensional representation of computed MEK (left) and MIBK (right) biofilm concentration profiles according the model (*1*). The polluted airflows from the right (inlet in layer 1) to the left (outlet from layer 10). The following quantities are represented vice versa: the interface equilibrium concentration, the liquid concentration in the first biofilm subdivision, in the second, third, and fourth subdivisions, and the concentration in the sorption volume. MEK and MIBK inlet concentrations, 0.30 and 0.33 g m^{-3}, respectively. (Top) airflow rate of 0.15 m^3 h^{-1}; (bottom) airflow rate of 0.34 m^3 h^{-1}.

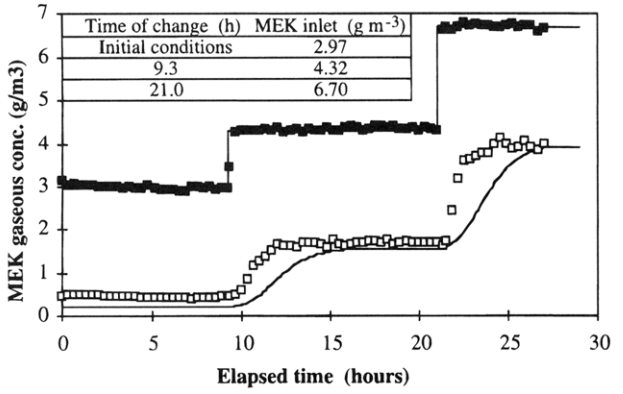

FIGURE 8. Dynamic response of the biofilter to step changes in MEK inlet concentration during MEK removal as a single pollutant at a volumetric loading of 44 m^3 m^{-3} h^{-1}. MEK inlet (■) and outlet (□) concentrations. The solid lines represent model predictions.

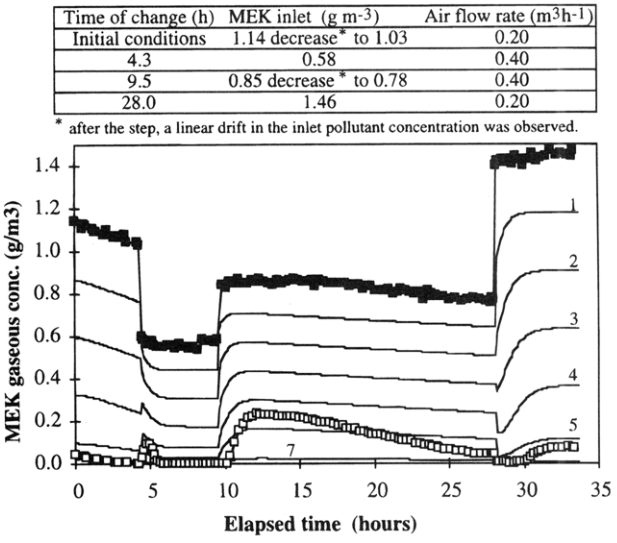

FIGURE 9. Dynamic response of the biofilter to step changes in both MEK inlet concentrations and airflow rates during MEK removal as single pollutant. MEK inlet (■) and outlet (□). The lines represent model predictions numbered for each layer in the biofilter height: 1 is the first layer, 2 is the second layer, etc.

capacity was recovered. This phenomenon can be explained on the basis that with increases in the flow rate and decreases in the inlet concentration the direction of the diffusion flux in the biofilm is reversed. Desorption occurs because the biofilm concentration becomes temporarily greater than the equilibrium value and because the process culture is unable to degrade the substrate at a higher rate than its diffusion rate. The temporary concentration increase, particularly in the third and fourth layer and to

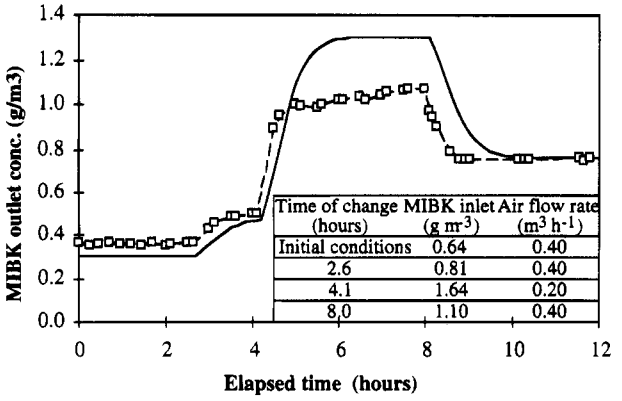

FIGURE 10. Dynamic response of the biofilter to step changes in MIBK inlet concentration and airflow rate during MIBK removal as single pollutant. Outlet concentration (--□--) and model prediction (solid line) are reported.

a lesser extent in the other layers, shows that the model effectively predicts such behavior.

After the second step change at 9.5 h, continuous MEK breakthrough was observed even when the inlet concentration was decreased linearly after the main step increase. However, the decrease observed in the outlet concentration was significantly more pronounced than that in the inlet concentration. This is due to increasing biodegradative activity in the lower parts of the biofilter, which were not normally exposed to MEK for extended periods and which required a period for adaptation for the biomass reactivation. The comparison of the slopes of the model computations for this period confirms the assumption that some biodegradative activity developed between 12 and 28 h.

Directly after the last combined flow–concentration step change at 28 h, the outlet concentration fell rapidly from 0.04 g m^{-3} to zero. The cause of this is clearly the intense sorption of pollutant in the upper part of the biofilter, which results in depletion in the lower part of the biofilter. This behavior is reflected by the simulated response of layers 3–5, which are subject to a significant decrease before the predicted increase occurs. After a few hours, a significant breakthrough was observed experimentally, and a new steady state was established.

Similar experiments were performed with MIBK as the sole pollutant. Typical results are presented in Figures 10and 11. In Figure 10, only outlet concentrations and model predictions are reported, and as noted previously, a short adaptation time was necessary to reach a new steady state. The modeled dynamic response of the biofilter is in relatively good agreement with the experimental results, except at the highest concentration where a ca. 25% deviation in the stationary performance is observed.

As discussed earlier for MEK, a temporary decrease in the outlet concentration after the second step increase, as shown in Figure 11, is predicted because of the combined flow rate decrease and inlet concentration increase. However, this behavior was not observed experimentally. As in Figure 10, good agreement is found between the experimental results and the computed values.

The model computations for the last two step changes are examined with respect to the local gaseous concentrations in Figure 12 where a typical response for a series of perfectly mixed reactors exposed to a step change can be recognized throughout the biofilter height. The delay involved in the propagation of the step change is intensified by the pollutant sorption/desorption properties of

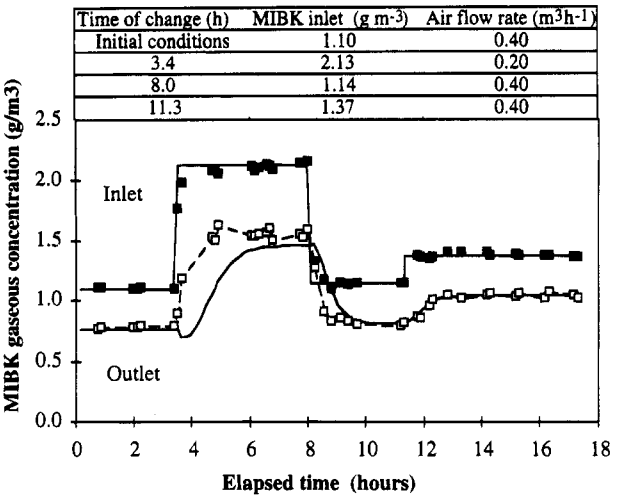

FIGURE 11. Experimental inlet (■) and outlet (--□--) concentrations, and modeled outlet responses (solid lines) for the biofilter subjected to both step changes in MIBK inlet concentrations and airflow rates.

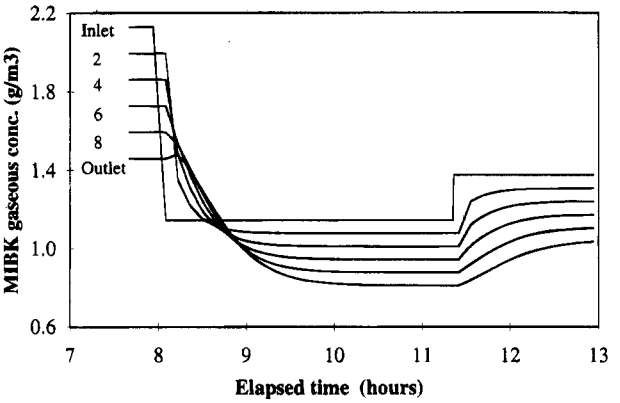

FIGURE 12. Simulated MIBK local gaseous phase concentrations in the inlet, second, fourth, sixth, eighth, and tenth (outlet) layers, during step changes. The responses are more gradual in the deeper layers. Steps as inset in Figure 11.

the packing. Design experiments which accurately define the pollutant/packing interaction are required to improve the reliability of the model for use during dynamic simulation.

The experiments reported in this section illustrate the response of biofilters to step changes in inlet conditions during the elimination of MEK and MIBK as single pollutants. The model developed proved effective for most of the predicted situations encountered, but deviation between experiments and model simulations were sometimes observed, particularly in the high sensitivity domain, i.e., close to breakthrough. Nevertheless, examination of the simulated dynamic concentration changes at different biofilter heights allowed the observed phenomena to be understood.

Combined MEK and MIBK Step Changes. Step changes during the removal of mixtures of MEK and MIBK are complex because of the interdependency of the biodegradation of the two ketones upon each other. However, they reflect practical situations and as a result present the greatest challenge with respect to modeling.

During the experiment illustrated in Figure 13, both the airflow rate and the inlet concentration of MEK were kept constant at 0.20 m^3 h^{-1} and 1.60 g m^{-3} respectively, while changes in MIBK inlet concentration were conducted in a stepwise manner.

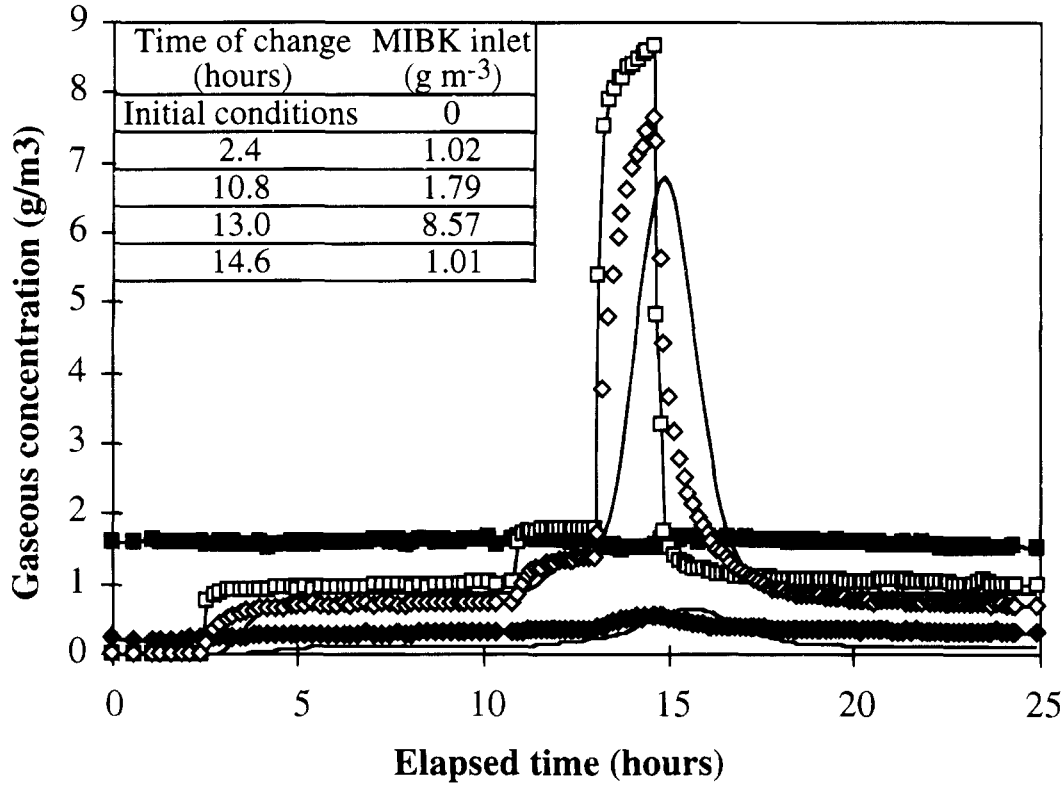

FIGURE 13. Dynamic response of the biofilter to step changes in MIBK inlet concentrations, at a volumetric loading of 44 $m^3 m^{-3} h^{-1}$. MEK inlet (■) and outlet (♦), MIBK inlet (□) and outlet (◇). The solid lines represent outlet concentrations predicted by the model.

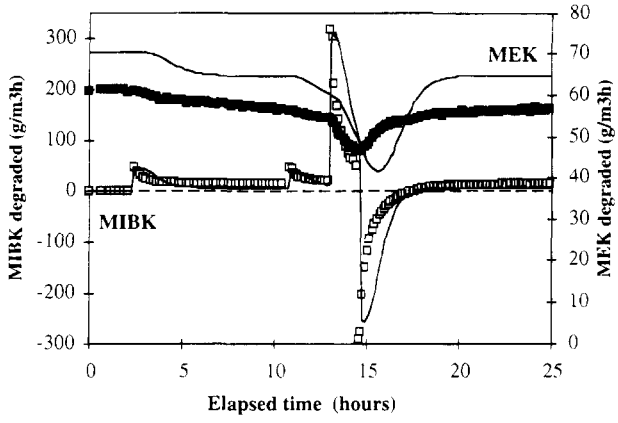

FIGURE 14. Elimination capacity for MEK (■, right-hand scale) and MIBK (□, left-hand scale) compared with model predictions (solid lines) during step changes in MIBK inlet concentration. Negative values for MIBK elimination are caused by significant desorption of MIBK from the packing. Steps according to the inset in Figure 13.

The results reported in Figures 13 and 14, with respect to elapsed time, are compared with predictions from the dynamic model. The first step change, at 2.4 h, corresponded to the introduction of MIBK into the inlet airstream. Immediately after the step change, sorption onto the packing played a major role, and the apparent elimination capacity was enhanced until equilibrium was reached. Rapid establishment of a steady state was achieved, but with only partial removal of MIBK. Little effect on MEK removal was observed, with only a decrease of ca. 7% in elimination capacity.

In the second step at 10.8 h, the MIBK inlet concentration was essentially doubled. Marked influences on its outlet concentration and on its elimination capacity, which increased from 13 to 19 $g m^{-3} h^{-1}$, were observed, indicating that the experiment was performed below the critical loading for the biofilter.

The third step at 13 h, which gave a final MIBK inlet concentration greater than 8 g m^{-3}, represents extreme operating conditions for biofiltration. A rapid increase in MIBK outlet concentration was observed, and due to sorption onto the packing, its elimination capacity reached apparent values as high as 300 $g m^{-3} h^{-1}$. However, overall performance changed before the establishment of a steady state with MEK elimination showing a marked drop from 55 to 47 $g m^{-3} h^{-1}$. Nevertheless, insignificant deactivation of the process culture was observed, and the system recovered its previous level of activity within a few hours of the last step change. After the last step change, the apparent elimination as strictly defined was negative because of MIBK desorption.

Model predictions show reasonable agreement as can be seen from both Figures 13 and 14. Detailed examination of Figure 13 shows that MEK elimination was overestimated, except during the major increase in MIBK concentration after 13 h. For such extreme operating conditions, deviations between model prediction and experiments can be expected. Nevertheless, globally the model predictions are reasonable and permit further elucidation of the phenomena involved.

The stagewise structure of the model considered for finite differencing (*1*) allows interpretation of computed local data. As far as local biodegradation rates are concerned, Figure 15 indicates a complex time course for modeled rates in the first biofilm subdivision of the first, fifth, and tenth layers of the biofilter. Initially, when no MIBK is present, MEK is degraded at the maximum value (V_m) in the upper part of the biofilter while toward the bottom virtual depletion occurs and the degradation rate is essentially zero. Introducing MIBK at 2.4 h markedly reduces

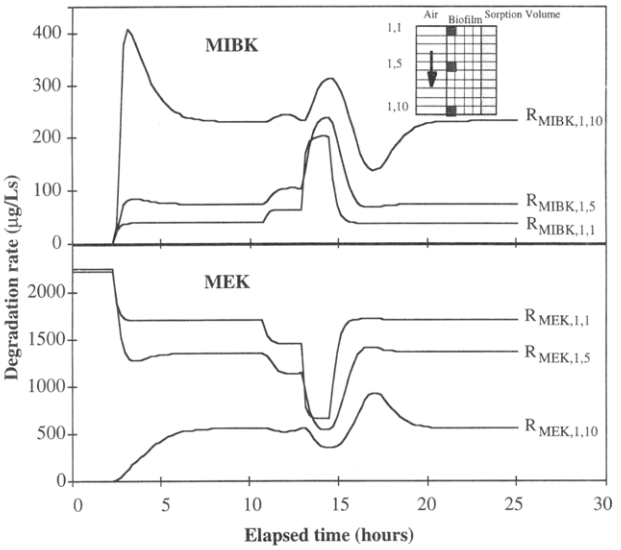

FIGURE 15. Modeled time course for MEK and MEK local biodegradation rates in the first biofilm subdivision for different filter heights, in the first layer $R_{s_{1,1}}$, in the fifth layer $R_{s_{1,5}}$, and in the tenth layer $R_{s_{1,10}}$. Maximum biodegradation rates (V_m) are 2240 and 551 $\mu g\ L^{-1}\ s^{-1}$ for MEK and MIBK, respectively. Steps according to inset in Figure 13.

the MEK degradation rate in the upper part of the biofilter, whereas deeper MEK penetration into the column leads to a significant increase in the MEK degradation rate in the tenth layer.

Over the whole time course, MIBK degradation rates are found to be higher in the bottom part (outlet end) than in the upper part (inlet end) of the biofilter. This is due to the interaction between MEK and MIBK degradation, which decreases as MEK moves down the column.

Until sorption equilibrium is complete between 2.4 and 4 h, a temporary maximum in the local MIBK degradation rate is observed after 3 h for the tenth layer. During this period, the bottom part of the filter behaves as a system for only MIBK removal, and the degradation rate achieved almost equals the V_m value.

The rest of the time course shows that the higher the MIBK inlet concentrations are, the higher the MIBK degradation rates are with coincident reductions of MEK biodegradation rates. However, the model predicts complex dynamic responses, such as a local maximum in MEK and a local minimum in MIBK degradation rates after 17 h in the tenth layer. Such detailed understanding of the interactions is impossible from steady-state models.

Transient experiments in biofilters provide valuable information for the behavior of such systems under practical operating conditions. They also help to develop an understanding of pollutant removal and permit the establishment of a knowledge base that is presently lacking in the literature. Step changes both in pollutant concentration and/or in flow rate demonstrate that the biofilter adapted rapidly to the new operating conditions. During transient-state operation, MEK/MIBK interactions and sorption/desorption processes were shown to play important roles. In most cases, the biofilter dynamic model proved effective in describing the phenomena observed. Examination of local gaseous and liquid concentrations as well as local degradation rates permitted an explanation of the complex events occurring under transient state operating conditions to be developed.

Conclusions

Experimental evaluation of a novel model for the description of gaseous waste biofiltration has been presented and discussed. The aerobic biodegradation of MEK and MIBK vapors from waste air served as the model system to illustrate the possibilities of the biofilter model. The use of pollutant mixtures provided much greater opportunity for developing an understanding of the process than did the use of single pollutants. Further, this reflects real situations.

The biofilter model (*1*) proved adequate for predicting most steady-state and dynamic situations over a wide range of sensible operating conditions. On the basis of model predictions, clear distinction was possible between the kinetic regimes that occurred under different operating conditions, thereby justifying the use in the biofilter model of nonlinear biodegradation kinetics. As far as steady-state performance was concerned, the model compared reasonably well for both single and dual pollutant removal characteristics and served as a basis for the comprehensive discussion of biofilter operation. The study of concentration profiles emphasized the fact that biofilters for polluted air treatment are complex bioreactor systems that require detailed definition, particularly when the removal of multiple pollutants is considered.

The description and discussion of dynamic phenomena proved useful, and new data concerning the transient response of biofilter reactors exposed to perturbations was presented. Step changes in airflow rate and/or in pollutant concentration(s) emphasized the major influence of sorption phenomenon during biofilter operation. After perturbation, a new steady state was usually reached within 2–5 h. When the two pollutants were removed as mixtures, marked influences of the compounds on each other's removal rates were observed, with MIBK being particularly adversely affected by the presence of MEK. The close interdependency of individual pollutant removal rates observed in all biofiltration experiments performed with mixtures of MEK and MIBK is expected to be the result of both mutual enhancement of pollutant toxicity and inhibition of individual pollutant degradation by each other.

The main differences between experimental observations and model predictions occurred when the model was applied to the removal of mixtures of MEK and MIBK. This emphasized the necessity for improved definition of the elimination kinetics of pollutants in biofilters, in particular, more appropriate quantification of the inhibition kinetics of mixed MEK/MIBK biodegradation. Further definition of the interaction(s) between the pollutant(s) undergoing treatment and the biofilter packing material is (are) also required in order to improve the dynamics of biofilter operation.

Acknowledgments

Our thanks are due to Prof. J. R. Bourne for providing the facilities in which this study was undertaken.

Nomenclature

C_j	(kg m^{-3}) gaseous concentration of component j
D_j	($m^2\ s^{-1}$) effective diffusion coefficient of component j
G	($m^3\ s^{-1}$) airflow rate

H_j	Henry coefficient of component j
$K_{i_{j \text{ on } t}}$	(kg m^{-3}) competition inhibition constant of component j on component t
K_{m_j}	(kg m^{-3}) Michaelis–Menten constant of component j
mc	biofilter packing moisture content (in wt %)
MEK	methyl ethyl ketone
MIBK	methyl isobutyl ketone
N	number of biofilm subdivisions in each layer (here $N = 4$)
n	biofilm and sorption volume subdivisions ($1 \leq n \leq N + 1$)
R_{s_j}	(kg m^{-3} s^{-1}) degradation rate of component j
$S_{j,n,w}$	(kg m^{-3}) liquid concentration of component j, subdivision n, layer w
t	(s, h) time
V	(m^3) total reactor volume
V_m	(kg m^{-3} s^{-1}) maximum degradation rate
W	number of layer subdivisions (here $W = 10$)
w	biofilter layer subdivisions: $1 \leq w \leq W$
Z	(m, μm) biofilm thickness (sorption volume not counted)

Greek Symbols

ϵ	porosity of filter bed

Literature Cited

(1) Deshusses, M. A.; Hamer, G.; Dunn, I. J. *Environ. Sci. Technol.* **1995**, *29*, 1048–1058.
(2) Deshusses, M. A.; Dunn, I. J. In *Proceedings of the 6th European Congress in Biotechnology*; Florence, Italy, June 13–17, 1993; Alberghina, L., *et al.*, Eds.; Elsevier Science Publishers B. V.: Amsterdam, The Netherlands, 1994; pp 1191–1198.
(3) Deshusses, M. A. Ph.D. Dissertation, Swiss Federal Institute of Technology Zurich, Switzerland, 1994.
(4) Deshusses, M. A.; Hamer, G. *Bioprocess Eng.* **1993**, *9*, 141–146.
(5) Shareefdeen, Z.; Baltzis, B. C.; Oh, Y.-S.; Bartha, R. *Biotechnol. Bioeng.* **1993**, *41*, 512–524.
(6) Mills, E. J.; Vernon, T.; Stack, T. In *Proceedings of the 8th industrial waste conference*; West Lafayette, IN, May 1953; Purdue University: Lafayette, IN, 1953; pp 492–517.
(7) Price, K. S.; Waggy, G. T.; Conway, R. A. *J. Water Pollut. Control Fed.* **1974**, *46*, 63–77.
(8) Govind, R.; Lai, L.; Dobbs, R. *Environ. Prog.* **1991**, *10*, 13–23.
(9) Kirchner, K.; Schlachter, U.; Rehm, H. J. *Appl. Microbiol. Biotechnol.* **1989**, *31*, 629–632.
(10) Wolff, F. *Biologische Abluftreinigung mit suspendierten und immobilisierten Mikroorganismen*; Reihe 15 Nr. 94; VDI Verlag: Duesseldorf, Germany, 1992; 140 pp.
(11) Tautz, H.; Bronnenmeier, R.; Frank, P.; Zeller, B. *Hochleistungsbiofilter*; Vortragsunterlagen zum Seminar Mikrobiologische Verfahrenstechniken zur Umweltsanierung; Wuppertal, June 4–5, 1992; W Linde AG: Germany, 1992; 16 pp.
(12) Zuber, L.; Dunn, I. J. Presented at the ECB6 conference, Florence, Italy, June 13–17, 1993; Poster WE 207.

Received for review August 8, 1994. Revised manuscript received December 15, 1994. Accepted December 16, 1994.[⊗]

ES940506F

[⊗] Abstract published in *Advance ACS Abstracts,* February 1, 1995.